THE ASTROPHYSICAL JOURNAL, 261:439–456, 1982, October 15

ROTATIONAL PROPERTIES OF 23 Sb GALAXIES

VERA C. RUBIN,[1,2] W. KENT FORD, JR.,[2,3] AND NORBERT THONNARD
Department of Terrestrial Magnetism, Carnegie Institution of Washington
AND
DAVID BURSTEIN[4]
National Radio Astronomy Observatory[5]
Received 1982 February 16; accepted 1982 April 27

ABSTRACT

We have obtained major axis spectra for 23 Sb galaxies in a sample chosen to encompass a wide range of radii, masses, and luminosities. These are generally field galaxies of high inclination, and our spectrograms extend, on the average, to about three quarters of the isophotal radius, R_{25}. The Sb rotation curves exhibit many of the systematic trends with luminosity shown by the Sc's studied previously. Velocities in small, low-luminosity, low-mass Sb galaxies rise gently to a maximum rotational velocity in a large fraction of their isophotal radius; velocities in large, high-luminosity, high-mass Sb galaxies reach their (higher) rotational velocity in only a small fraction of their isophotal radius. However, rotational velocities span a range of higher values for Sb than for Sc galaxies.

Correlations exist between velocity extrapolated to the isophotal radius $V(R_{25})$ and radius, and between $V(R_{25})$ and blue absolute magnitude M_B, i.e., the conventional Tully-Fisher relations, but with two major differences. (1) The regression line for Sb galaxies is displaced ~ 0.1 dex from that for Sc's. At equal luminosity, the rotational velocity of an Sb galaxy is about 25% larger than that of an Sc. At equal rotational velocity, an Sb is both smaller and less luminous than an Sc. (2) The mean slope of the $V(R_{25})$ versus M_B relation is steep (~ -10) for both Sb and Sc galaxies, even with blue magnitudes. We discuss reasons why we believe both of these effects are real. Only the correlation of radius with blue luminosity is independent of Hubble type. From these relations it follows that the ratio of the dynamical mass (assumed spherical) interior to the isophotal radius, to the blue luminosity is independent of blue luminosity, for a given Hubble type. The geometrical mean value is $\langle \mathfrak{M}(R_{25})/L_B \rangle = 2.6 \pm 0.2$ for 20 Sc's; $\langle \mathfrak{M}(R_{25})/L_B \rangle = 4.4 \pm 0.4$ for 23 Sb's. And for the set of 11 Sa's we are presently studying, $\langle \mathfrak{M}(R_{25})/L_B \rangle = 6.1 \pm 0.7$. These results imply that the Hubble sequence is a two-parameter sequence in which the dominant parameters can be grouped as Hubble type and luminosity [or $V(R_{25})$, or R_{25}, or mass, or density]. Of these latter parameters, it is likely that density is the most fundamental.

Subject headings: galaxies: internal motions — galaxies: structure

I. INTRODUCTION

As a continuation of our program to study the rotational properties of the disks of spiral galaxies, we present here observations of 23 Sb galaxies. These galaxies were chosen: (*a*) to be well classified (generally in the Revised Shapley-Ames Catalog [RSA] [Sandage and Tammann 1981]); (*b*) to be of relatively high (generally $i > 50°$) inclination; (*c*) to have angular diameters of a few arc minutes; (*d*) to span the largest range of luminosity and radius which we could find, and (*e*) not to be strongly barred. The resulting sample of Sb's are relatively isolated galaxies, with a few being possible members of small groups.

Along with the rotation curve data for the Sb galaxies, we derive in this paper relations among the integral properties of mass, luminosity, radius, and rotation velocity for these galaxies. These integral relations are then compared with those similarly derived for an

[1]Visiting Astronomer, Cerro Tololo Inter-American Observatory, supported by the National Science Foundation under contract AST 78-27879.
[2]Visiting Astronomer, Kitt Peak National Observatory, which is operated by the Association of Universities for Research in Astronomy, Inc., under contract with the National Science Foundation.
[3]Visiting Astronomer, Lowell Observatory.
[4]Guest Investigator, Palomar Observatory, which is operated by the California Institute of Technology.
[5]Operated by Associated Universities, Inc., under contract with the National Science Foundation.

analogous set of Sc galaxies (Rubin, Ford, and Thonnard 1980 [Paper I]; Burstein *et al.* 1982 [Paper II]).

Results for several of the galaxies have been presented earlier (NGC 7217: Peterson *et al.* 1978; NGC 1620, 2590: Rubin, Ford, and Thonnard 1978; NGC 3067: Rubin, Thonnard, and Ford 1982). Four galaxies classified Sbc are also included in the group, but their physical properties do not distinguish them from the Sb's.

II. COMPILATION OF THE BASIC DATA

a) The Observations

The galaxies included in this study are listed in Table 1, arranged by increasing luminosity. Spectrograms of high dispersion and at high spatial scale were obtained for each galaxy, with the slit of the spectrograph aligned along the major axis. Spectrograms along the minor (or other) axis were also obtained for 12 of these galaxies. The majority of the spectra were taken with the RC spectrographs of the Cerro Tololo and the Kitt Peak 4 m telescopes, generally at 25 Å mm^{-1} and 25″ mm^{-1}. A few spectrograms were taken at 50 Å mm^{-1}. Several spectra were also obtained with the spectrograph of the 100 inch (2.5 m) du Pont telescope at Las Campanas. For these spectra, the dispersion and scale are 63 Å mm^{-1} and 52″ mm^{-1}, respectively. All three spectrographs incorporate RCA C33063 Carnegie image tubes, and the final phosphor was imaged onto IIIa-J plates which had been baked in forming gas and preflashed. Exposure times were generally 2^h to 3^h for the major axis plates, and less for the minor axis (for lack of telescope time). Slit position angles are listed in column (5) of Table 1; major axes (col. [6]) are marked D if they are determined dynamically from velocities in two or more position angles. Otherwise they come from measurements of the Palomar Observatory Sky Survey (POSS) prints. The adopted inclinations are listed in column (7).

Reproductions of all of the galaxies and of the major axis spectra are shown in Figure 1 (Plates 4–7). The photographs come from a variety of sources, including plates taken with an image tube camera at the Lowell 42 inch (1.1 m) telescope and at the 72 inch (1.8 m) telescope of the Ohio State and Ohio Wesleyan Universities at Lowell Observatory, and plates taken for surface brightness studies with the Palomar 1.2 m Schmidt.

b) Measurement of the Spectra

All spectra were measured on a Mann two-dimensional measuring machine at the Department of Terrestrial Magnetism by Rubin. Hα and [N II] lines were routinely measured, but [S II] lines were measured only if Hα and [N II] were confused with night sky emission. Generally, night sky OH lines were used for wavelength standards and to map the curvature; new wavelengths for the OH lines come from Brault and Hubbard (1981). For a few of the spectra taken early in the program, neon comparison lines were used to establish the rest frame. Velocities are calculated in the optical convention: $V = cz = c(\lambda - \lambda_0)/\lambda_0$.

For each galaxy, the measured heliocentric velocities V_0 on the plane of the sky are shown in Figure 2, as a function of angular distances from the nucleus. Velocity undulations extending about 10 km s^{-1} are assumed to be real, although occasionally they arise in the process of taking the mean of the two sides of the major axis. The center of symmetry of the velocities is adopted as the heliocentric velocity of the galaxy (Table 1, col. 3). The agreement of this optical velocity with 21 cm velocities is excellent. For 15 of these Sb galaxies, we have 21-cm velocities from observations at NRAO and Arecibo.[6] The difference $\Delta V = V_{opt} - V_{21}$ is small; $\Delta V = -3 \pm 10(1\sigma)$ km s^{-1}. A detailed comparison of optical and 21 cm velocities for the Sa, Sb, and Sc galaxies in our study is currently under way (Thonnard *et al.* 1982).

c) Basic Data for the Sb Galaxies

The physical data for the Sb galaxies are given in Table 1, and are defined in the same manner as for the Sc sample (Papers I and II). A distance for each galaxy (col. [4]) is obtained from the central velocity corrected for the motion of the Sun with respect to the Local Group, $\Delta V = 300 \cos b \sin l$. We adopt $H = 50$ km s^{-1} Mpc^{-1} throughout. None of the galaxies are in large, prominent clusters, but a few are in some of the small groups identified by de Vaucouleurs (1975). Galaxies in these groups are noted in Table 1, as are galaxies with a close neighbor. Mean velocities of the groups were formed from the velocities included in the Rood (1980) galaxy velocity catalog. Two galaxies, NGC 1356 and 4448, have central velocities more than 50 km s^{-1} from the mean velocities of their groups. They are assigned the group distance using the mean velocity of the group.

Column (8) lists the radius of the galaxy, R_{25}, to the 25th B mag per square arcsec isophote as given by de Vaucouleurs, de Vaucouleurs, and Corwin (1976 [RC2]). Emission lines have been detected and measured, on the average, to 76% of R_{25}. Column (9) lists the linear radius of each galaxy, $R_{25}^{i,b}$, derived from RC2 and from the adopted distance, and corrected for the effects of galactic extinction and internal extinction as in Paper I. The radius of the farthest measured velocity, R_f, is listed in column 10, and the ratio of $R_f/R_{25}^{i,b}$ is given in column (11). Only for four galaxies is the radial coverage less than 70%.

[6]The Arecibo Observatory is part of the National Astronomy and Ionosphere Center, which is operated by Cornell University under contract with the National Science Foundation.

TABLE 1

PARAMETERS FOR PROGRAM Sb GALAXIES[a]

NGC (1)	Class RSA (2)	$V_\odot$ (km s^{-1}) (3)	Distance (Mpc) (4)	Observed Position Angles (5)	Line of Nodes (degrees) (6)	Inclination (degrees) (7)	R_{25} (arcmin) (8)	$R_{25}^{i,b}$ (kpc) (9)	R_{farthest} kpc (10)	$R_f/R_{25}^{i,b}$ (11)
4800	Sb(rs) II–III	891	19.5	24.8	25	53	0.89	4.9	4.0	0.81
2708	SASb: (a)	1985	35.5	28, 118	28	61	1.48	14.7	10.4	0.71
3067	Sb(s) III	1456	28.3	100, 105	102D	68	1.23	9.6	7.3	0.76
4448	Sb(r) I–II	657	19.0	93.9	94	69	1.99	11.0	7.0	0.64
1515	Sb(s) II	1162	19.1	14	14	81	2.69	13.6	11.4	0.84
1353	Sbc(r) II	1517	30.0	138	138	65	1.69	14.0	8.1	0.58
1325	Sb	1591	30.0	52	52	70	2.29	18.8	14.5	0.77
7537	SBTb (a)	2675 (c)	57.3	78.9	79	79	1.17	18.3	17.3	0.95
U11810	Sb (b)	4709	98.3	175	175	74	1.3	34.0	24.2	0.71
7171	Sb(r) I	2727	57.4	114	122	52	1.38	23.9	15.0	0.63
7217	Sb(r) II–III	955 (c)	24.7	9 pos.angles	86	35	1.86	15.1	10.5	0.70
1620	SATbc(a)	3490 (c)	68.4	25, 115	23.7D	69	1.51	29.8	22.8	0.77
3054	SBbc(s) I	2425	43.1	22, 112	114D	50	1.95	25.7	22.8	0.89
2590	Sb(b)	4985 (c)	95.8	76.8, 167	76.8D	75	1.5	39.6	18.0	0.45
2815	Sb(s) I–II	2542	45.5	13	13	72	1.77	26.5	20.1	0.76
1417	Sb(s)I.3	4114	81.5	2, 92	2.5D	50	1.41	33.7	26.5	0.79
1085	SAb(a)	6784	136.	6, 15, 105	15D	38.7	0.87	34.8	25.5	0.73
7083	Sb(s) I–II	3092	59.6	14, 102	11D	51	2.23	39.0	34.1	0.87
U12810	Sb(b)	8124	165.	55	55	70	1.1	51.4	51.8	1.01
3145	SBbc(rs) I	3671	68.8	23, 113	23D	61	1.66	33.8	25.4	0.75
3223	Sb(s) I–II	2900	52.4	40, 310	130D	52	2.04	34.8	24.9	0.72
7606	Sb(r) I	2237	47.5	63, 150	150D	66	2.88	39.8	31.9	0.80
3200	Sb(r) I	3516 (c)	65.3	348	348	72	2.39	46.0	39.8	0.87

[a] Col. (1) U = Uppsala General Catalog (Nilson 1973; UGC). Col. (2), classification from RSA (Sandage and Tammann 1981); (a) from RC2 (de Vaucouleurs, de Vaucouleurs, and Corwin 1976); (b) from UGC. Col. (3), night sky OH lines used for velocity standards; wavelengths from Brault and Hubbard 1981 except for (c), which use comparison neon lines. Velocity is center of symmetry of rotation curve. Col. (4), distance $= (V_\odot + 300 \sin l \cos b)/H$; $H = 50$ km s^{-1} Mpc^{-1}, except for NGC 4448 and 1353, which are group distances. Col. (6), D denotes line of nodes determined dynamically from plates in two or more position angles. Col. (7), b/a from RC2; $\cos i = [1.042 b^2/a^2 - 0.042]^{1/2}$, except NGC 4800 (measured) and NGC 7217 (Peterson *et al.* 1978). Col. (8), radius in arcmin from RC2, to 25 mag arcsec^{-2}; for UGC galaxies, R_{25} obtained from RC2 relation. Col. (9), $\log R_{25}^{i,b} = \log R_{25} - 0.07 \log a/b - \log (1 - \Delta m_b/3.35)$ to correct radius for internal and galactic extinction effects (Paper I).

NOTES FOR INDIVIDUAL GALAXIES

NGC 4800.—Filamentary arm structure, strong Hα and [N II] emission continuous to large radial distance. Inclination = 53° adopted from measures of ellipticity on POSS.

NGC 4448.—High surface brightness galaxy. Strong nuclear emission; extremely weak emission beyond nucleus. Member of nearby group (G13, Coma I cloud; de Vaucouleurs 1975) with $\langle V \rangle = 950 \pm 200$ km s^{-1} from 24 members.

NGC 2708.—Intense nuclear emission.

NGC 3067.—Complex nuclear structure. Narrow nuclear emission. Spectrum of 3C 232, at distance 113″, shows absorption due to foreground H I with $V_{\text{gal}} - V_{\text{cloud}} = 36$ km s^{-1} (Haschick and Burke 1975; Rubin, Thonnard, and Ford 1982).

NGC 1353.—Strong narrow nuclear emission with large velocity gradient. Narrow Na D stellar absorption lines whose nuclear velocity gradient is about one-third that of emission lines. Member of Eridanus group (G31; de Vaucouleurs 1975) with $\langle V \rangle = 1500 \pm 190$ km s^{-1} from 19 members.

NGC 1515.—Filamentary arm structure. Strong, narrow emission in nuclear region; weak knotty emission in disk. Inner velocity peak near 1 kpc rises to 233 km s^{-1}. Sharp, narrow stellar Na D absorption lines show nuclear velocity gradient about one-fourth that of emission lines. Small low surface brightness companion is background galaxy with velocity near 15000 km s^{-1}.

NGC 1325.—Small nucleus, filamentary arm structure. Very weak nuclear emission; strongest Hα observed in knot at large radial distance. Sharp Na D stellar absorption lines show smaller velocity gradient than in gas emission.

NGC 7537.—Pair with Sc galaxy NGC 7541 at about one diameter; $V_c(7541) = 2685$ km s^{-1}. Both are likely foreground galaxies superposed on the Peg I cluster. Weak nuclear continuum; strong emission. Form of rotation curve is completely normal, but blue luminosity of galaxy is excessively high for the observed rotational velocity (Fig. 6*a*), perhaps due to recent interaction-induced star formation.

UGC 11810.—Two-armed global spiral pattern. Galaxy #187 in Sc I sample of Rubin *et al.* 1976.

NGC 7171.—Spectrum taken in PA = 114° to avoid star. Intensity of [N II] = Hα in nucleus.

NGC 7217.—Filamentary, tightly wound spiral arms, big bulge galaxy. Studied earlier (Peterson *et al.* 1978) in detail. Inner velocity peak at 2 kpc with $V = 289$ km s^{-1}. Strong nuclear stellar continuum; strong nuclear emission with [N II] stronger than Hα. Velocity gradients ~ 50 km s^{-1} across arms.

NOTES FOR INDIVIDUAL GALAXIES—*Continued*

NGC 1620.—Weak nuclear continuum and weak nuclear emission, with [N II] = Hα in nucleus. Well defined velocity gradient in nucleus.

NGC 3054.—Multiarmed spiral with small nucleus and inner ring. Intense nuclear stellar continuum (overexposed). Emission knotty across arms, with large velocity gradients.

NGC 2590.—Broad nuclear emission, with [N II] = Hα; weak disk emission.

NGC 2815.—Strong stellar continuum; broad nuclear emission with [N II] = Hα. Weak disk emission. Broad velocity peak near 4 kpc with $V = 292$ km s^{-1}.

NGC 1417.—Strong nuclear stellar continuum; broad nuclear emission.

NGC 1085.—Strong nuclear stellar continuum (overexposed).

NGC 7083.—Attractive spiral. Strong nuclear stellar continuum (overexposed); weak disk emission.

UGC 12810.—Filamentary spiral arms with weak nuclear stellar continuum. Several distinct strong emission knots in nucleus; Hα stronger than [N II].

NGC 3145.—Attractive spiral with strong nuclear stellar continuum; strong nuclear emission with large velocity gradient. [N II] probably stronger than Hα in nucleus. Illustrated in Hubble Atlas (Sandage 1961).

NGC 3223.—Filamentary arm spiral with strong nuclear stellar continuum; strong nuclear emission with large velocity gradient. [N II] probably stronger than Hα in nucleus. Large velocity gradients across arms.

NGC 7606.—Multiarm spiral with very weak nuclear emission. Emission weak beyond nucleus, but increasing in intensity with increasing radial distance. Broad velocity peak near 12 kpc with $V = 273$ km s^{-1}.

NGC 3200.—Attractive spiral with strong nuclear stellar continuum; strong nuclear emission with large velocity gradient. Velocity gradients ~ 50 km s^{-1} across arms. Inner velocity maximum near 2 kpc. Overall appearance of rotation curve suggestive of that for our Galaxy.

Integral properties derived from the observed quantities are given in Table 2 for these Sb galaxies. Apparent blue magnitudes are taken from the RC2 or, when not available, from the Uppsala General Catalog (Nilson 1973 [UGC]). Corrections to apparent magnitude for galactic extinction, Δm_b (col. [4]) are derived by the method of Burstein and Heiles (1978, 1982). Corrections for internal extinction to face-on magnitudes, $\Delta m_i = 1.90 \log (a/b)$ (col. [5]) come from the work of Burstein (1982*b*). The constant in the magnitude correction for internal extinction is the same as that adopted for the Sc galaxies. This seems valid, for the bulge and internal extinction properties of the Sb and Sc galaxies are not dramatically different. It is important to point out, however, that adoption of a smaller internal extinction for the Sb's would not be sufficient to account for the differences between Sb and Sc galaxies which we discuss below. The corrected apparent magnitude $m_c^{i,b}$ is given in column (6), and the resulting absolute blue magnitude in column (7).

Two characteristic rotation velocities are given for each galaxy. The velocity V_f measured at the final observed point is given in column (8); the velocity extrapolated to the isophotal radius, $V(R_{25})$, is given in column (9). Because we have observed to 76% of the galaxy disks in the mean, and rotation curves are rising only slowly in their outer regions, the extrapolation from $V(R_f)$ to $V(R_{25})$ is not large. However, our extrapolation is very conservative, so the maximum rotational velocity may be higher for some galaxies than that given in column (9). The few galaxies which exhibit a high peak in the velocities at small radial distance are identified in the notes. As in Paper II, we employ $V(R_{25})$ as a measure of the "rotational velocity" of a galaxy in this paper. This measure is representative of the global properties of the galaxy, and is equivalent to the 21 cm profile width. For the 15 Sb galaxies that have good 21 cm observations, the mean difference between the profile width at half-intensity divided by 2 sin i, $V_{0.5}$, and $V(R_{25})$ is small: $[V(R_{25}) - V_{0.5}] = +8 \pm 19 (1\sigma)$ km s^{-1}.

Radial velocities for 16 of these galaxies are listed in RC2 (in addition to NGC 7217, whose velocity comes from the present data). The mean of the absolute value of the difference $\langle |\Delta V| \rangle = \langle |V_{\rm RC2} - V_{\rm here}| \rangle$ is 81 km s^{-1}. For the Sc galaxies in Paper I, the velocity difference was also 81 km s^{-1}. For the 18 galaxies in common with the Rood (1980) velocity catalog, the agreement is better, $\langle |\Delta V| \rangle = 35$ km s^{-1}, as new velocities of higher accuracy replace those in older catalogs.

While no quantitative measure of the emission lines in these spectra have yet been made, their qualitative appearance differs from that of the Sc's. The emission line characteristics indicate that they arise in larger bulged, less knotty galaxies than the Sc's. With increasing luminosity there is generally an increasingly strong red stellar continuum in the nucleus; the ratio of nuclear [N II] to Hα increases. Beyond the nucleus the ratio of emission line strength to the continuum strength (averaged over a few angstroms) is usually small. This is in marked contrast to most Sc spectra, in which the ratio of emission line strength beyond the nucleus to the continuum strength is large. For many of the Sb spectra, the bulge region beyond the nucleus has weak or absent emission; no such regions are seen in the Sc spectra. Moreover, in the Sb's the emission beyond the bulge tends to be fairly continuous or weakly knotty, while in the Sc's the emission is generally a string of discrete knots. (In the Sa's, the bulge region lacking emission generally incorporates an even larger fraction of the galaxy radius.) These spectroscopic properties may be distinctive enough to make possible a morphological

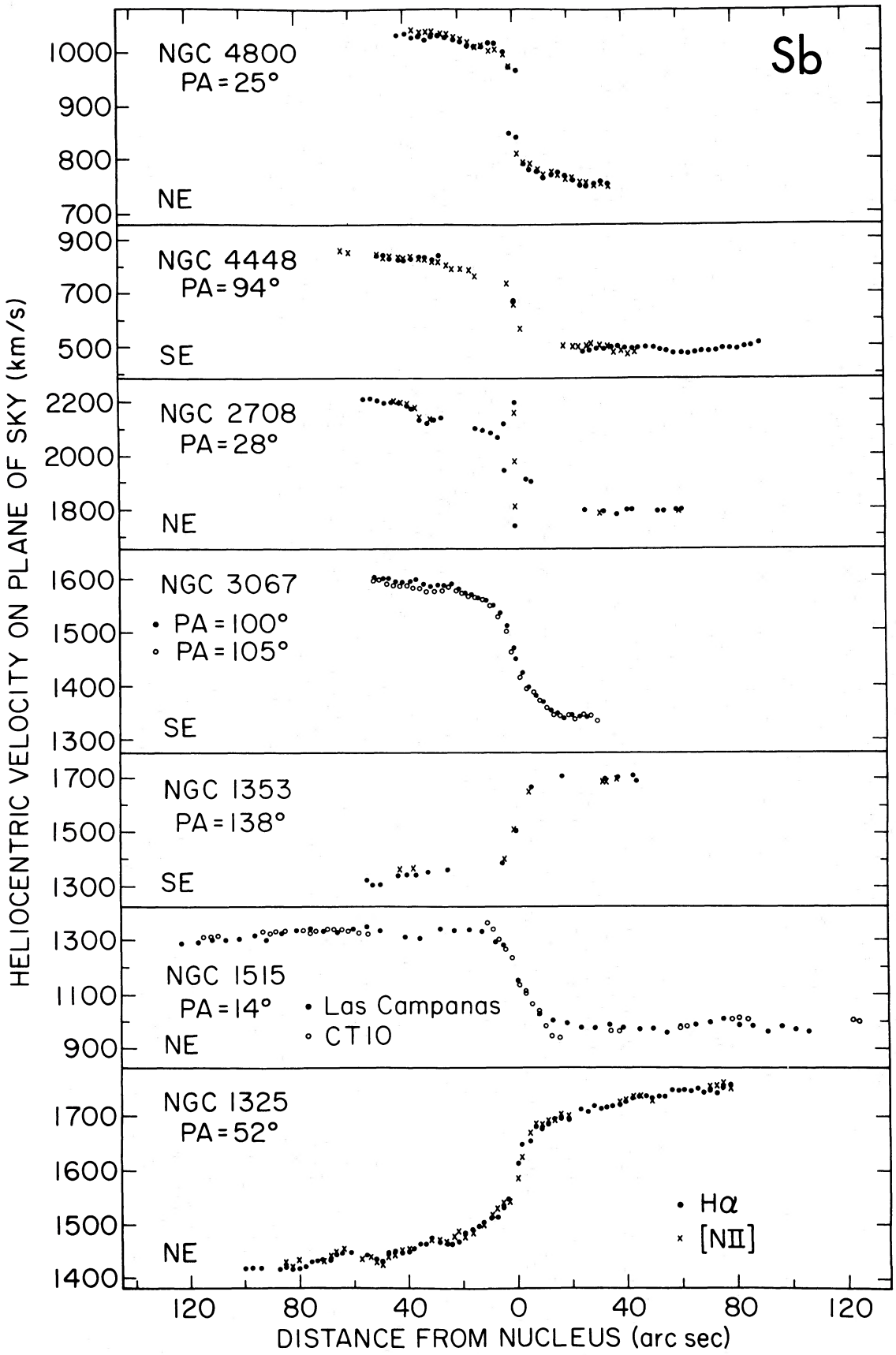

FIG. 2*a*

FIG. 2.—Heliocentric line-of-sight velocities on the plane of the sky as a function of angular distance from the nucleus for 23 Sb galaxies

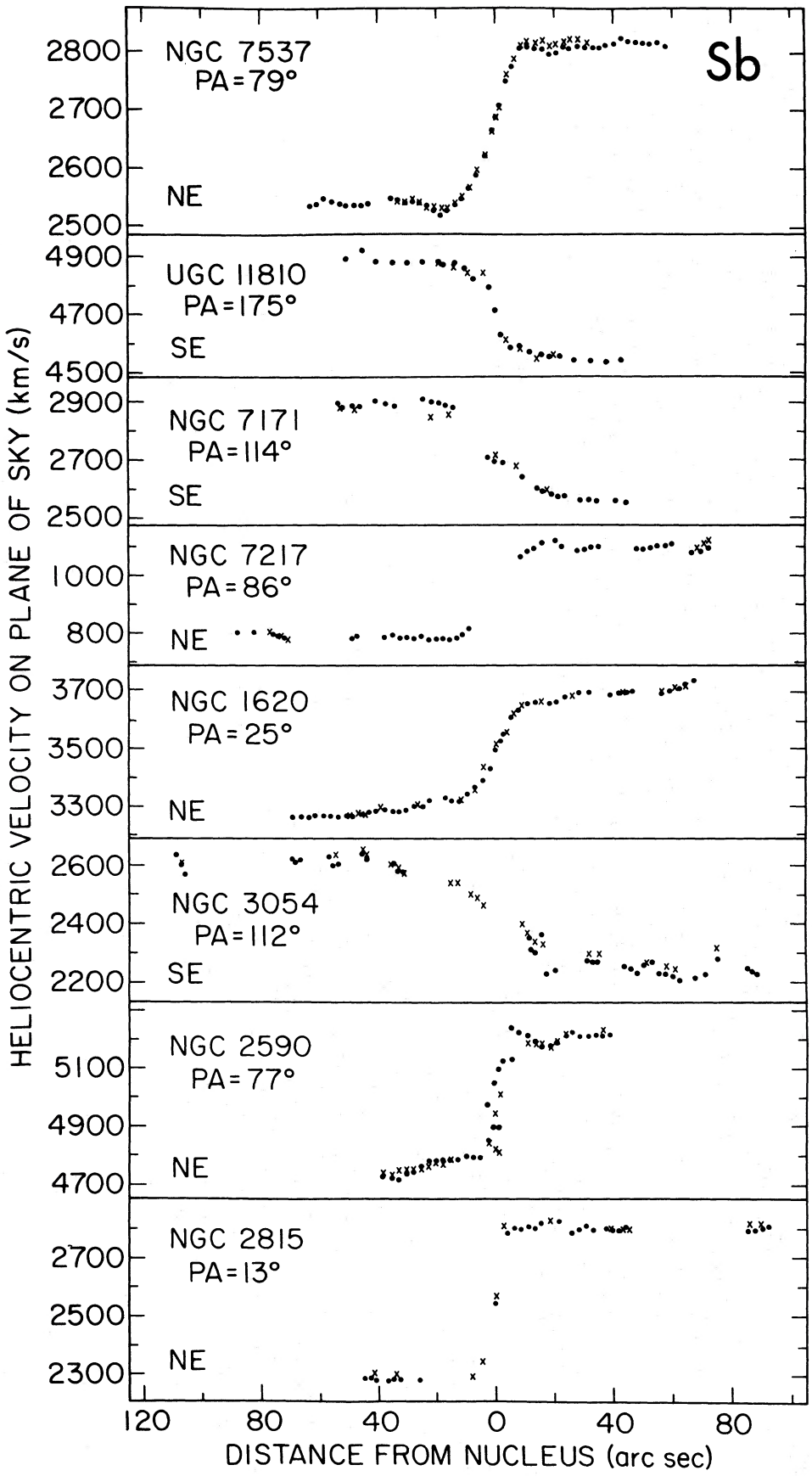

FIG. 2*b*

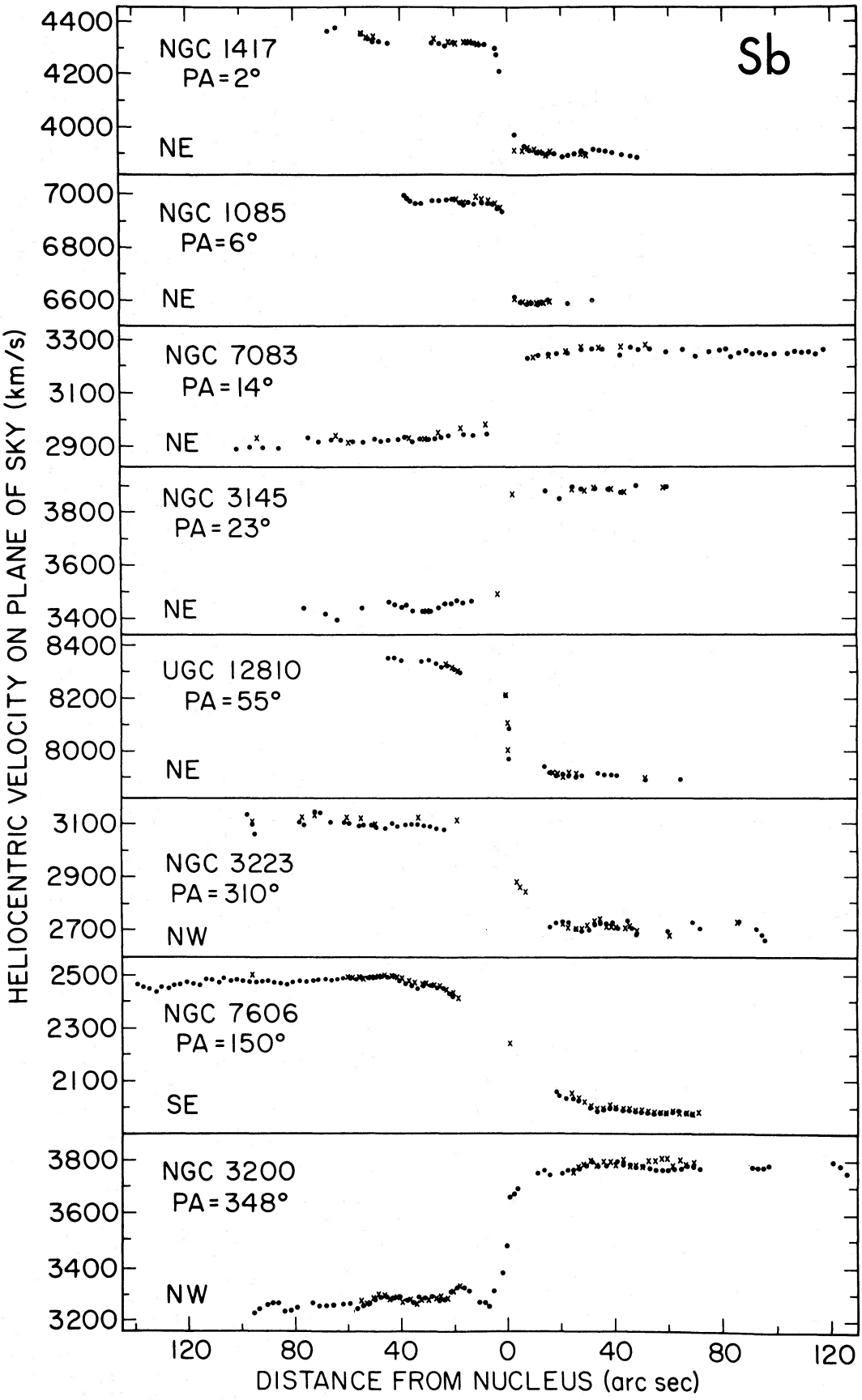

FIG. 2c

TABLE 2

MAGNITUDES, VELOCITIES, MASSES, AND $\mathfrak{M}/L$ RATIOS FOR PROGRAM Sb GALAXIES[a]

Name NGC (1)	Distance (Mpc) (2)	B_T (mag) (3)	Δm_b (mag) (4)	Δm_i (mag) (5)	$m_c^{i,b}$ (mag) (6)	M_B (mag) (7)	$V(R_f)$ (km s^{-1}) (8)	$V(R_{25}^{i,b})$ (km s^{-1}) (9)	$\mathfrak{M}(R_{25})$ ($10^{10}\,\mathfrak{M}_\odot$) (10)	$\mathfrak{M}(R_{25})/L$ (solar units) (11)
4800	19.5	12.30	0.0	0.39	11.91	−19.55	175	179	3.65	3.39
2708	35.5	(13.6)	0.02	0.54	13.0	−19.8	241	241	19.9	15.4
3067	28.3	12.70	0.05	0.72	11.93	−20.33	150	161	5.78	2.74
4448	19.0	12.0	0.29	0.74	11.0	−20.4	190	190	9.24	4.29
1515	19.1	11.83	0.0	1.14	10.69	−20.72	155	153	7.41	2.45
1353	30.0	12.25	0.02	0.64	11.59	−20.80	226	226	16.6	5.12
1325	30.0	12.32	0.02	0.78	11.52	−20.87	184	184	14.8	4.27
7537	57.3	13.80	0.07	1.05	12.68	−21.11	141	144	8.83	2.04
U11810	98.3	(14.7)	0.04	0.91	13.8	−21.2	187	197	30.7	6.53
7171	57.4	13.00	0.22	0.38	12.40	−21.39	213	213	25.2	4.50
7217	24.7	11.10	0.41	0.13	10.56	−21.40	258	254	22.7	4.02
1620	68.4	(13.6)	0.19	0.74	12.7	−21.5	248	252	44.0	7.10
3054	43.1	12.13	0.25	0.34	11.54	−21.63	239	239	34.2	4.90
2590	95.8	(14.0)	0.10	0.94	13.0	−21.9	252	256	60.4	6.75
2815	45.5	12.66	0.59	0.82	11.25	−22.04	280	280	48.3	4.74
1417	81.5	12.75	0.13	0.34	12.28	−22.28	328	330	85.4	6.72
1085	136.	(13.6)	0.11	0.19	13.3	−22.4	310	310	77.8	5.48
7083	59.6	12.00	0.13	0.36	11.51	−22.37	222	222	44.7	3.24
U12810	165.	(14.4)	0.11	0.78	13.5	−22.6	235	235	66.0	3.87
3145	68.8	12.35	0.20	0.54	11.6	−22.58	273	275	59.5	3.49
3223	52.4	11.79	0.45	0.38	10.96	−22.64	254	255	52.6	2.97
7606	47.5	11.55	0.18	0.66	10.71	−22.67	246	246	57.4	3.15
3200	65.3	12.29	0.27	0.82	11.20	−22.87	282	282	85.1	3.89

[a] Col. (3), B_T from RC2, except Zwicky magnitude (in parentheses) for those lacking B_T. Col. (4), Δm_b from method of Burstein and Heiles 1978. Col. (5), $\Delta m_i = 1.9 \log a/b$. Col. (8), velocity at last measured point, corrected for relativistic redshift $1/(1+z_0)$, and slightly smoothed. R_f is listed in Table 1, col. (10). Col. (9), velocity extrapolated conservatively to R_{25}. Col. (11), $M_B(\odot) = 5.48$.

type–luminosity classification scheme for galaxies based on spectral appearance alone. A more complex spectral classification scheme has been used by Morgan (1959) and his colleagues, from observations of a broader spectral region at much lower dispersion.

III. THE ROTATION CURVES OF Sb GALAXIES

We assume that the emission lines in the Sb galaxy spectra come from H II regions which are moving in planar circular orbits about the center of each galaxy. These circular velocities are derived from the measured rotation velocities, the adopted major axis (Table 1, col. [6]) and the adopted inclination (col. [7]). The rotation curve is formed using velocities from both sides of the major axis; velocities are generally symmetrical about the central velocity. The principal exceptions to this symmetry are NGC 3054, 3223, and 3200. The adopted rotation curves are listed in Table 3, and are plotted to the same linear scale in Figure 3.

The Sb rotation curves exhibit many of the same systematic trends with luminosity and with mass as those shown by the Sc curves (Paper II). Generally, all curves rise to velocities near the maximum velocities in a few kiloparsecs from the nucleus; virtually all curves are flat or slowly rising at large nuclear distances. Furthermore, it is clear from Figure 3 that the form of the rotation curve is a luminosity characteristic for the Sb galaxies. Small, low-luminosity, low-mass Sb galaxies have velocities which rise to lower maximum velocities than do the large, high-mass, high-luminosity galaxies, and the maximum velocity is reached in a larger fraction of the galaxy isophotal radius. Large, high-luminosity Sb's reach their (higher) rotational velocity in only a small fraction of their isophotal radius. This systematic progression of rotational properties (and hence local mass or local density distribution) with the integral mass interior to the isophotal radius suggests that the local distribution of mass is tightly coupled with the total mass of the galaxy.

To illustrate the very systematic nature of the rotation curves, we compare the rotation curves for 4 Sb galaxies in Figure 4. The radial scale is in units of the isophotal

TABLE 3

ROTATIONAL VELOCITIES IN PLANE OF GALAXY (km s^{-1})

NGC	RADIUS (kpc)																										
	0	0.5	1.0	1.5	2	3	4	5	6	8	10	12	14	16	18	20	22	24	26	28	30	32	34	40	45	50	51.8
4800.....	...	130	148	149	160	172	175																				
2708.....	...	65	92	112	124	...	187	188	195	235	241																
3067.....	0	59	89	105	119	127	128	138	143	(149)																	
4448.....	...	...	...	132	153	178	189	190	190	(190)																	
1515.....	0	124	199	232	233:	212:	185	162	175	159	156	(155)															
1353.....	0	...	168	...	186	188	189	190	195	226																	
1325.....	0	56	77	92	103	120	134	134	146	160	162	183	184														
7537.....	0	33	60	88	109	132	140	140	138	136	130	142	139	(184)													
U11810.....	0	...	81	106	120	123	129	142	152	162	166	170	172	134	(141)												
7171.....	0	25	50	70	89	133	179	198	204	213	213	213	213	174	176	180	184	187	(187)								
7217.....	...	...	220	257	282	276	268	269	269	263	258	(258)		(213)													
1620.....	0	56	94	117	132	158	178	176	173	194	216	213	215	232	234	237	246	(248)									
3054.....	0	28	50	72	92	126	155	180	193	209	223	241	255	253	246	240	239	(239)									
2590.....	...	...	150:	187	207	217	218	214	206	203	211	225	239	251	252												
2815.....	...	...	256	268	275	282	292	289	273	269	271	...	...	...	...	280											
1417.....	...	...	153	240	246	243	261	270	273	275	266	261	258	265	274	286											
1085.....	...	...	...	256	272	290	305	312	311	305	299	303	314	309	305	300	297	302	310								
7083.....	...	...	...	...	173	183	179	194	200	210	216	220	220	219	215	212	213	218	222	222	222	222	222				
U12810.....	0	92	104	...	...	...	...	...	...	...	(184)	191	200	206	213	216	218	220	221	222	223	223	224	227	221	231	238
3145.....	...	...	212	...	...	...	...	237	235	248	262	262	246	251	260	264	267	271	(273)								
3223.....	...	...	40	60	...	...	224	235	239	245	246	249	251	253	253	253	253	254	(254)								
7606.....	...	...	...	...	...	...	...	(210)	227	256	273	273	273	270	258	255	264	270	268	253	239	238					
3200.....	0	119	180	224	254	262	243	223	225	247	258	262	264	265	267	270	272	275	278	279	281	282	...	282			

NOTE.—Velocities here corrected for relativistic Doppler effect $1/(1+z_0)$. Parentheses indicate that final velocity occurs before tabulated R. R_f listed in Table 1, col. (10).

radius; this representation enhances the differences between low and high luminosity rotation curves. An examination of Figure 4 makes it clear that the rotational velocity is a good measure of a galaxy luminosity. These galaxies differ in luminosity by a factor of 10, yet the rotation curves for the big galaxies are approximately scaled-up versions of those for the small galaxies, when plotted in this manner. (Recall that when plotted on a linear scale, the linear extent of the approximately flat portion increases with increasing luminosity.) It is also clear from Figure 4 that other measures taken from the rotation curves can be equally useful as luminosity discriminants, i.e., the fractional radius where $V = 100$ km s^{-1} (Rubin, Burstein, and Thonnard 1980), or the velocity at any fractional radius (Thonnard, Rubin, and Ford 1981; Thonnard and Rubin 1981). We are presently attempting to determine the most profitable procedure for deducing spiral galaxy luminosities from their total rotational properties.

Rotational velocities span a range of higher values for the Sb than for the Sc galaxies. A set of rotation curves for the Sc's would look similar to Figure 4, except that each Sc rotation curve would lie lower than the Sb curve for a galaxy of equal luminosity. By the forms of their rotation curves (i.e., mass distributions), most Sb's and Sc's would be indistinguishable. The distribution of $V(R_{25})$ for the Sb and Sc program galaxies is shown in Figure 5*a*. The range in rotational velocity is 144–330 km s^{-1}, with a median velocity of 222 km s^{-1} for the Sb's, compared with a range of 99–304 km s^{-1} (or 248 km s^{-1} excluding the supergiant Sc, UGC 2885) and a median of 175 km s^{-1} for the Sc's. We caution, however, that as the Sb and Sc samples do not represent volume-limited samples, the median values are useful only as an indicator of the center of the largest range which we could uncover. Within the Sb class (and within the Sc class) rotational velocities are higher for higher luminosity galaxies. This correlation, the Tully-Fisher (1977) relation, is discussed in § IV below.

In Paper II we showed that virtually all of the Sc rotation curves could be modeled by a characteristic form, which in turn implied (or resulted from) a single characteristic mass distribution for Sc galaxies. The principal parameter of this mass distribution is a radial mass scale length. Mass scale length is inversely related to luminosity; mass scale zero points vary little with luminosity. Large Sc's have more mass contained within $R_{25}^{i,b}$ than small Sc's because their larger isophotal radii contain many more (smaller) mass scale lengths. Also of considerable importance, mass scale radii for Sc's vary (inversely) by only a factor of three, for a range of 15 in isophotal radius and 100 in luminosity.

A detailed comparison shows that many Sb's have mass distributions similar to those observed in the Sc's (Paper II), some perhaps with higher mass scale zero points. For the Sc's, we observe that rotational velocities are generally rising slightly in the range 1 to 25 kpc, $V(R) \propto R^{+0.1}$. From this observation and the definition of mass (eq. [1] below), it follows that the total mass interior to any R goes as $\mathfrak{M}(R) \propto R^{1.3 \pm 0.1}$, and local density averaged over a spherical shell falls as $\rho \propto R^{-1.7}$. For the Sb's we observe a similar velocity rise in the 1 to 25 kpc region, $V(R) \propto R^{+0.1}$, and a density fall, $\rho \propto R^{-1.8 \pm 0.1}$, excluding NGC 1515 which has a dramatically different rotation curve. Such uncharacteristic rotation curves imply that some Sb's have mass distributions different from the general form derived for the Sc's in Paper II. A detailed discussion of the mass distribution within spiral galaxies is deferred until the study of the companion sample of Sa galaxies has been completed.

IV. THE TULLY-FISHER RELATION FOR THE Sb GALAXIES

a) Comparison with Sc Galaxies

The correlations of M_B with $V(R_{25})$ and of $R_{25}^{i,b}$ with $V(R_{25})$, the conventional Tully-Fisher relations, are shown in Figures 6*a* and 6*b*. In making least squares linear fits, we continue the procedure followed in Paper II. When both variables are distance dependent, we compute the mean line (iterated to convergence); when one variable is distance independent, as $V(R_{25})$, then we prefer to use it as the dependent variable. However, we give both that slope and the mean slope as well. For the Sb sample, the least squares regression line of $V(R_{25})$ on M_B produces a steep slope of -15.0; the *mean* line has a slope of -10.0. We show in Figures 6*a* and 6*b* the least-squares fits for the Sb and Sc (Paper II) samples. It is evident that the zero points of both Tully-Fisher relations are different for the Sb's and the Sc's, but that steep slopes are common to both relations for both samples. [For the Sc's, the derived slopes of M_B versus $V(R_{25})$ are -14.3 and -11.5(mean).] For Sc and Sb galaxies, $R_{25} \propto V(R_{25})^{\sim 4}$. Although the increased scatter in the Sb data as compared with the Sc data places some points close to the Sc relation, at a given luminosity the values for each relation are well separated. For example, for galaxies with equal luminosities, i.e., equal radii, Sb rotation velocities are higher than those of Sc's by about 0.1 dex ($= 26\%$). At a mean absolute magnitude of $M_B = -21$, velocities are $V(R_{25}) = 209$ and 166 km s^{-1}, for an Sb and an Sc, respectively. Alternatively, for galaxies with equal rotation velocities, an Sb will be less than one-half as large and only one-fourth as luminous as an Sc galaxy. For an Sc galaxy to mimic the rotational properties of an Sb, it must be both larger and more luminous than the Sb.

b) Comparison with the Infrared Tully-Fisher Relation

These two results, a Hubble type separation in the Tully-Fisher relation and a steep slope for the correlation with blue magnitudes, contradict work by

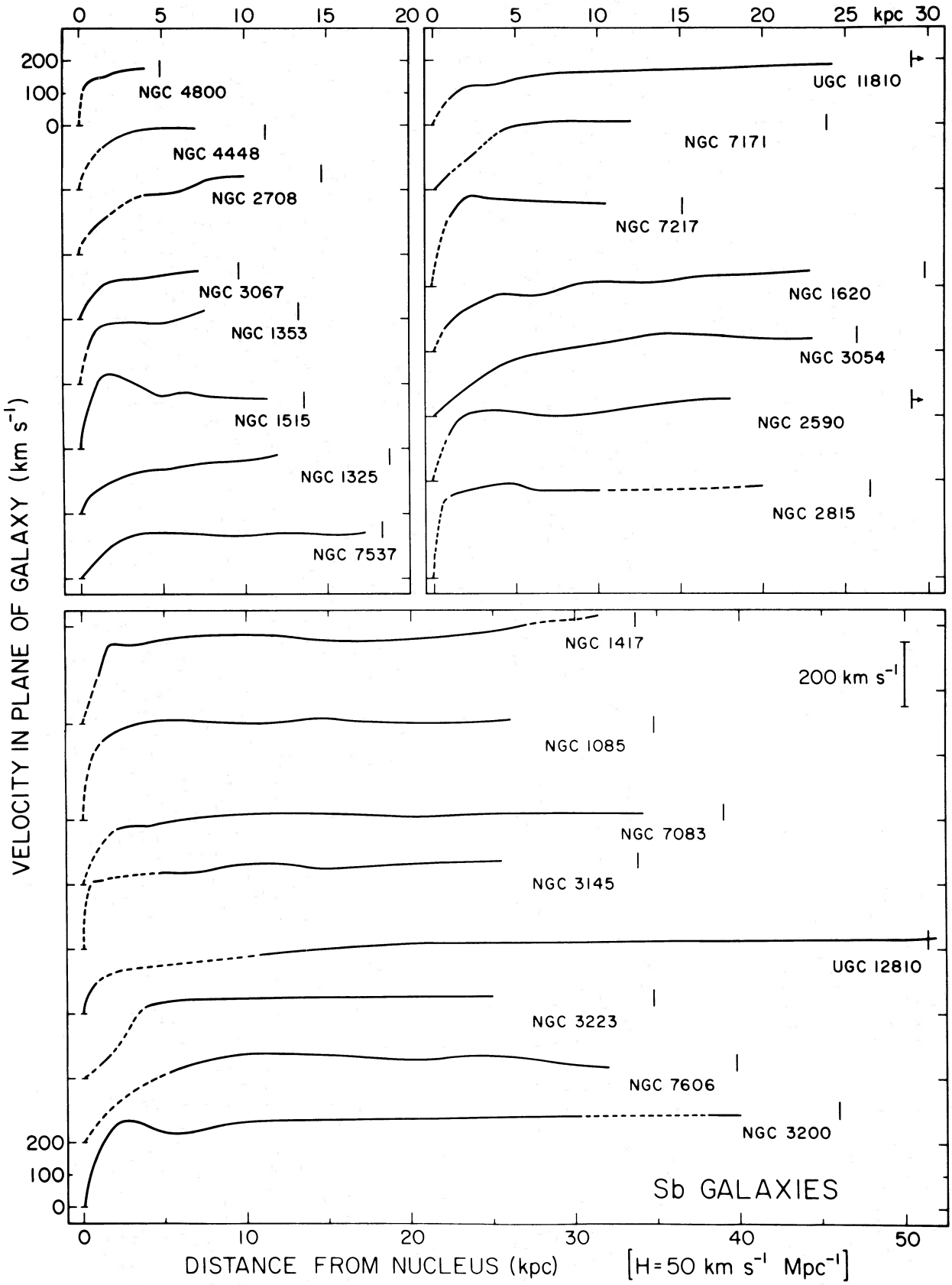

FIG. 3.—Mean velocities in the plane of the galaxy, as a function of linear radius for 23 Sb galaxies, arranged approximately according to increasing luminosity. Adopted curve is rotation curve formed from the mean of velocities on both sides of the major axis. Vertical bar marks the location of R_{25}, the isophote of 25 mag arcsec^{-2}, corrected for effects of internal extinction and inclination. Regions with no measured velocities are indicated by dashed lines.

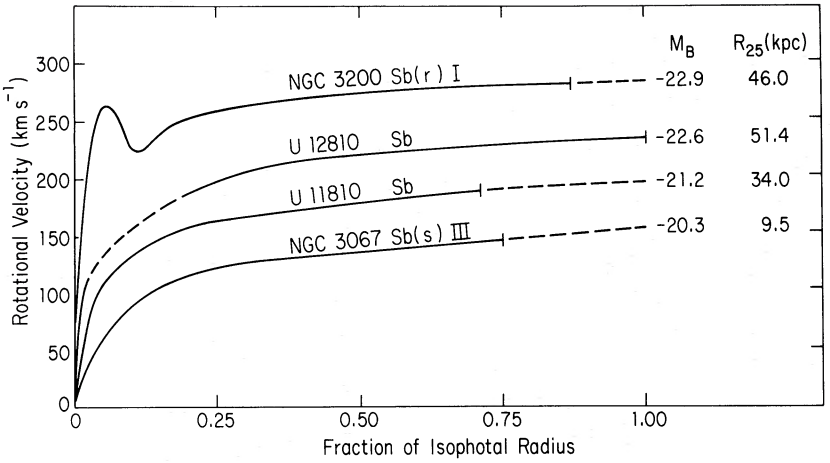

FIG. 4.—Rotation velocity for four Sb galaxies plotted as a function of the fraction of the isophotal radius, R_{25}, for each galaxy. With increasing luminosity, rotation velocities rise rapidly at a smaller fraction of R_{25}, rise to a higher velocity, and have a longer (both in the fractional and in the linear representations) nearly flat portion.

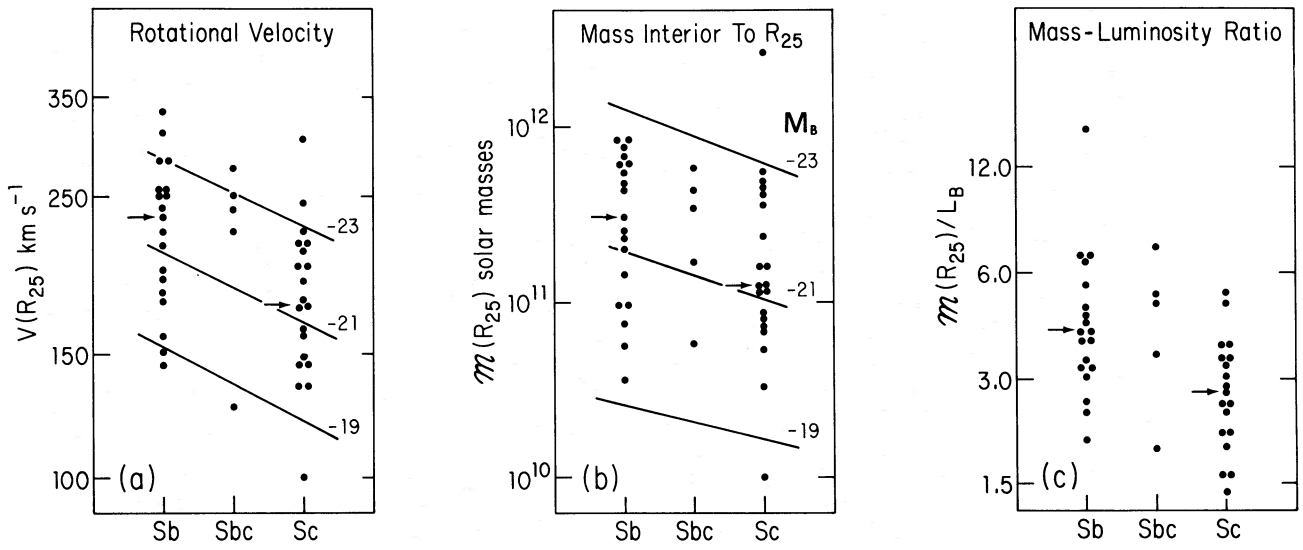

FIG. 5.—(*a*) Values of rotational velocity at the isophotal radius, $V(R_{25})$, as a function of Hubble type, for the galaxies of types Sb–Sc which we have studied. The median Sb and Sc values are indicated by arrows. (*b*) The same, for mass interior to the isophotal radius, $\mathfrak{M}(R_{25})$. At a given Hubble type, velocity and mass each increase with luminosity. Lines of constant luminosity (M_B) are indicated. (*c*) The same, for mass to blue light ratio, $\mathfrak{M}(R_{25})/L_B$. Within a given Hubble class, this ratio is not a function of luminosity. Note that the samples do not represent the distribution in a volume limited space, but instead mark the total range of parameters which we could detect.

Aaronson, Huchra, and Mould (1979 [AHM]) and Bottinelli *et al.* (1980). They have separately argued that a steep slope (~ -10) for the absolute magnitude-rotation velocity relations for spirals should exist only with near-infrared or infrared magnitudes; and AHM have shown that the zero point of their relation is independent of Hubble type. We now have two independent samples of field spirals for which we obtain a steep slope with blue magnitudes. Also, Weekes (1981) has observed a cluster sample for which he also derives a slope of -10 using broad-band R (5600–7600 Å) colors. We cannot identify any reasons why our selection procedures (i.e., covering the maximum range of luminosity we could find) should lead to a slope different from that obtained for a volume-limited sample.

Although infrared data are not yet available for most of the galaxies in our sample, three important points can be inferred from the mean colors as a function of Hubble type (Aaronson 1977, 1978; de Vaucouleurs 1977): (1) The use of infrared magnitudes defined on the AHM system will result in a Tully-Fisher relation with a slope at least as steep as obtained here. This is because

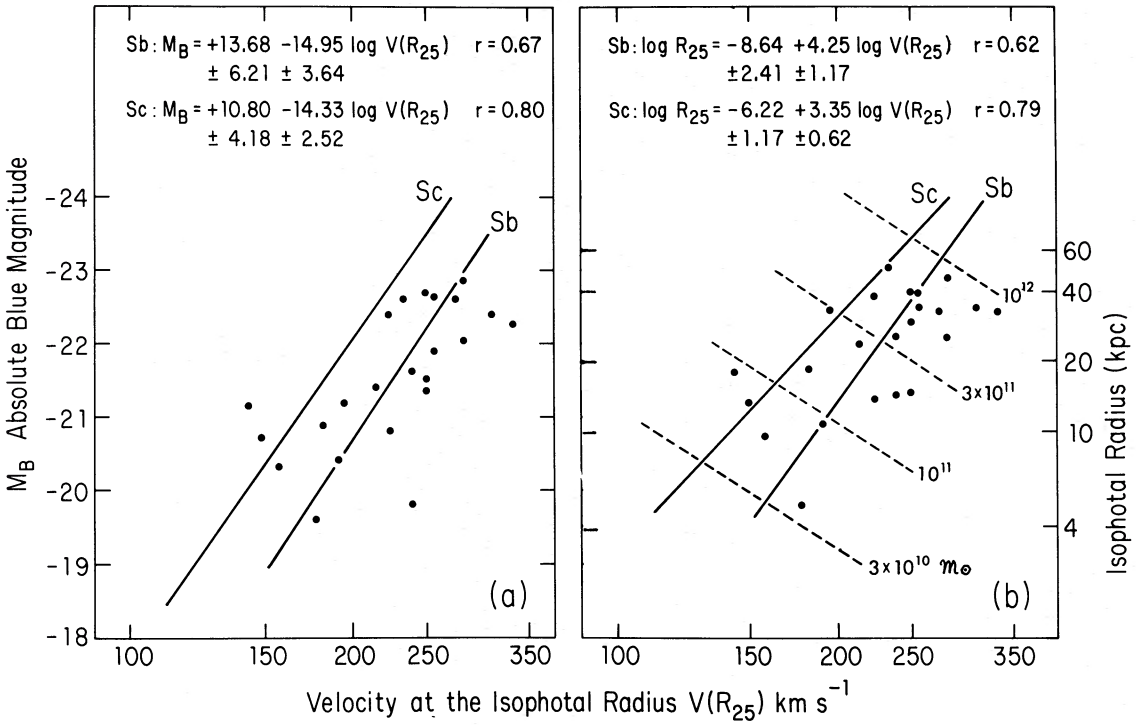

FIG. 6.—(*a*) Correlation of M_B with velocity at the isophotal radius $V(R_{25})$ for 23 Sb galaxies (*filled circles*). The least squares line is indicated. Also plotted is the least squares fit for 20 Sc galaxies studied earlier (Paper I). (*b*) Correlation of isophotal radius R_{25} with $V(R_{25})$. The corresponding line for the Sc's is shown. Loci of constant mass are indicated by the dashed lines. For an Sc to have a rotational velocity equal to that of an Sb, the Sc has to be both brighter and larger than the Sb.

any correlation of $B-H$ color with luminosity is likely to be in the sense of high-luminosity spirals being redder than low-luminosity spirals (e.g., Visvanathan 1981; Tully, Mould, and Aaronson 1982). (2) The zero point difference between the Sb's and the Sc's will probably be present in the infrared data as well. The mean $B-H$ colors obtained from the above sources indicate that Sb's on average are 0.3 mag redder than Sc's. While the sense of the difference is in the right direction, the size is a factor of 4 too small to eliminate the zero point difference seen in blue magnitudes. (3) The radius-rotation velocity version of the Tully-Fisher relation (Figure 6*b*) also shows a significant zero point difference between Sb's and Sc's. Since infrared magnitudes are currently measured in terms of optical radii, the zero point difference in Figure 6*b* will remain, regardless of the color of the magnitude system.

In order to see if either the zero point separation or the steep slope which we observe is an artifact of our sample, we have examined several questions:

1. Are the optical rotational velocities analogous to the 21 cm profile widths read at 20%, which the above authors employ? For the 15 Sb galaxies in our sample with good 21 cm profiles, the mean slope of the Tully-Fisher regression remains steep: -12.6 using the optically derived velocity, $V(R_{25})$, and -11.7 using the 21 cm profile widths, corrected for inclination. In addition, reading the 21 cm profile at 25%, 50%, or 75% of the peak intensity does not significantly alter the slope of the regression. Finally, for both Sb and Sc galaxies the 21 cm profile widths and the optical rotational velocities are in excellent agreement, so the Hubble type dependence remains, using any reasonable 21 cm value for V_{max}.

2. Does an all-sky value for the Hubble constant prejudice the results? The use of smooth Hubble flow models to obtain distances is an oversimplification, in view of the results of other investigations (Rubin *et al.* 1976; Aaronson *et al.* 1980, 1982; Davis *et al.* 1980). Both large scale motions and individual peculiar motions will affect the adopted distances, and hence the distribution of points on Figure 6. However, adopting the Virgo-centric flow model of Schechter (1980) for the Sb and Sc samples produces no significant difference in the Tully-Fisher correlation. Relatively few Sb or Sc program galaxies are at distances and directions where the Virgo flow is important. Even the Procrustean procedure of adopting $H=50$ km s^{-1} Mpc^{-1}, $V_c<3000$

km s^{-1}; and $H = 100$ km s^{-1}, $V_c > 3000$ km s^{-1} does not alter the slope (although it does decrease the correlation) of the Sb Tully-Fisher plot.

Unlike the Sc sample, which has a high correlation between luminosity and distance (because the galaxies were chosen principally by angular diameter to match the spectrograph slit), the Sb sample has a systematic effect only in that the lowest luminosity galaxies are nearby. Beyond about 1700 km s^{-1}, there is a good mix of luminosity and distance (correlation between log V_c and M_b is only 0.37 for 16 galaxies). This can be seen from Table 1, by noting that many galaxies of highest luminosity are of intermediate distance, while many galaxies of intermediate luminosity are at greatest distances. The Tully-Fisher relation for the 16 galaxies, $V > 1700$ km s^{-1}, retains a steep mean slope of -9.6, but a decreased correlation of only 0.5.

These considerations convince us that the differences between our results and those of AHM are due to real differences in the properties of our data samples. Our sample of spirals has a wide range of luminosities within a single Hubble class, which leads to a view of the Hubble sequence as at least a two-parameter family. AHM, and Tully, Mould, and Aaronson (1982) have large data sets in which Hubble type is correlated with luminosity (cf. Burstein 1982*a* for AHM), which leads them to infer that spiral galaxies form a one parameter sequence.

Our sample of Sb's was chosen to span the widest possible luminosity range within this Hubble type. The specific parameters which define the Sb sample—viz., apparent diameter, redshift, and inclination—do not vary systematically with Hubble class (e.g., de Vaucouleurs 1959). The galaxies are generally in the field or in loose groups. AHM and collaborators have chosen galaxies by very different criteria. Rotational velocities of their galaxies come from 21 cm profile widths. Hence their sample is restricted to galaxies with detectable neutral hydrogen. For equal hydrogen content, galaxies with narrow profiles (i.e., low rotational velocities) are more easily detected. Thus their sample selection involves criteria which *do* vary systematically with Hubble class: H I gas content and profile width (e.g., Roberts 1978). Additionally, their initial work was based on galaxies located generally in or around clusters of galaxies. The contradictions in our data samples may be enhanced by the very different selection criteria used. Differences between the physical properties and the range of physical properties as a function of Hubble type for field galaxies and cluster galaxies may also be important. It seems fair to say that the causes of the conflict between our results and the infrared–21 cm Tully-Fisher relations are not yet understood. Resolving these contradictions should lead to an increased understanding of galaxy systematics and dynamics.

c) *The Sources of Scatter in the Tully-Fisher Relations*

We can identify four possible sources of scatter in the Tully-Fisher relations, all of which may be influencing the distribution of points in Figures 6*a* and 6*b*:

1. Errors in rotation velocities due to incorrect inclinations. There may not be a simple one-to-one relation between b/a and inclination, as we assume.
2. An intrinsic difference in the zero point of the Tully-Fisher relations among galaxies of different Hubble types. Intermediate types will broaden the distribution.
3. Errors in the adopted distances, due to peculiar motions, and deviations from a smooth Hubble flow.
4. Errors in isophotal radius, due, e.g., to different zenith distances of different galaxies.

It is likely that all of these sources contribute to produce the scatter in Figures 6*a* and 6*b*. Errors in adopted distances or in apparent radii will produce errors in magnitudes and linear radii which are correlated; i.e., a galaxy that is overlarge will also be overbright. This is in fact observed, for the residuals in Figures 6*a* and 6*b* are correlated. It is of interest to note that the forms of the rotation curves are generally normal for the galaxies which show large scatter from the mean lines.

V. RADIUS, LUMINOSITY, AND INTEGRAL MASS RELATIONS

a) *The Radius-Luminosity Relation for Spiral Galaxies*

It is well known (e.g., de Vaucouleurs 1959) that there exists a close relationship between radii and luminosities of spiral galaxies that is essentially independent of Hubble type. Thus it comes as no surprise that for the Sb's, isophotal radius and blue luminosity not only are tightly correlated but also have nearly the same relationship as that for the Sc's. This is illustrated in Figure 7, which plots log $R_{25}^{i,b}$ versus M_B for both sets of galaxies.

The least squares fitted mean radius-luminosity relation for the Sb galaxies is $L_B \propto (R_{25}^{i,b})^{1.5 \pm 0.2}$, which is not significantly different from that obtained for the Sc galaxies (exponent 1.7 ± 0.1). For Sb as well as Sc galaxies in our sample, the mean blue surface brightness is lower for high-luminosity galaxies than for low-luminosity galaxies.

b) *Masses and Mass-to-Luminosity Ratios*

For each galaxy, the integral mass interior to R_{25}, $\mathfrak{M}(R_{25})$ (i.e., the disk plus halo mass), is determined assuming a spherical mass distribution and

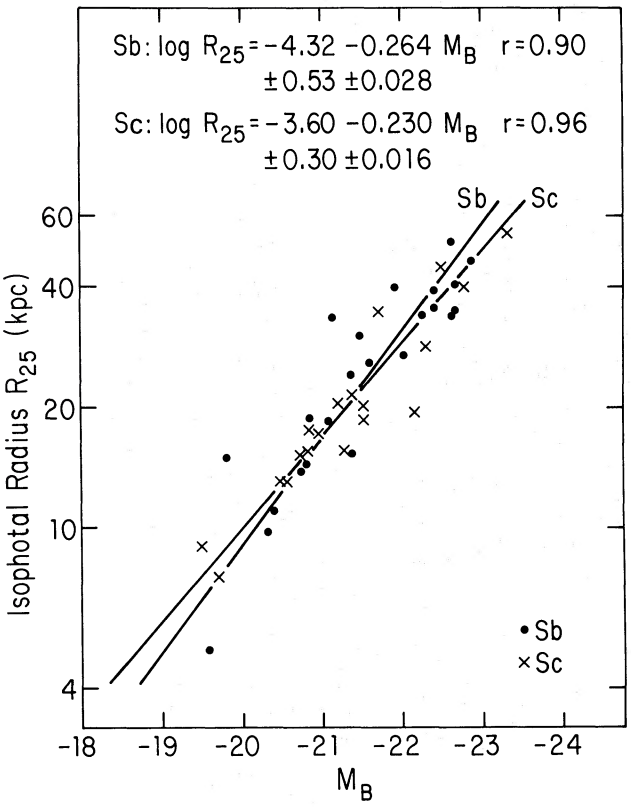

FIG. 7.—Correlation of isophotal radius, R_{25} with M_B, for both Sb and Sc galaxies. Note that the relation is independent of Hubble type.

Newtonian gravitational theory (Paper II),

$$\mathfrak{M}(R_{25}) = 2.326510^5 RV^2(R), \qquad (1)$$

where V is in km s^{-1}, and R is in kiloparsecs. The mass contained within the isophotal radius, $\mathfrak{M}(R_{25})$, is listed in Table 2, column (10). Masses interior to any other radius may be formed from the data in Table 3.

We have shown above that an Sb and an Sc of the same size will have the same luminosity, but that the Sb will have a higher rotational velocity by 0.1 dex (26%). Hence from equation (1), the Sb will have a mass higher by V^2, or 0.2 dex (58%). The range of masses encompassed by the Sb sample is compared with that of the Sc sample in Figure 5*b*. From the forms of the rotation curves, it follows that an *Sb has a higher density at every nuclear distance than an Sc of equivalent luminosity*.

However, the Hubble sequence cannot be defined by density alone, for a high-luminosity Sc will have a rotational velocity, and hence mass and density, higher than that of a low-luminosity Sb. This dependence on luminosity within a Hubble class implies that Hubble type plus at least one additional parameter are needed to specify general properties of a galaxy. This result is not new, but has been stated in a variety of ways (Brosche 1973; Bujarrabal, Guibert, and Balkowski 1981; Whitmore 1982). The correlations we observe suggest that the second parameter may be luminosity (van den Bergh 1960, 1961) or any of the parameters closely related to luminosity: radius, or V_{max}, or velocity at a specified isophotal radius, or mass, or density. Among these parameters, it seems likely that density is the most fundamental.

The correlation of mass with luminosity, $\mathfrak{M}(R_{25})$ versus M_B, is plotted in Figure 8 for the Sb galaxies. As indicated by the lines of constant mass-to-light ratio, most Sb's have mass-to-blue luminosity ratios $[\mathfrak{M}(R_{25})/L_B]$ between 3 and 7; the full range is 2 to 15 (Table 2, col. [11], and Fig. 5*c*). The geometric mean $\mathfrak{M}(R_{25})/L_B$ for the Sb's is 4.4±0.4. For comparison,

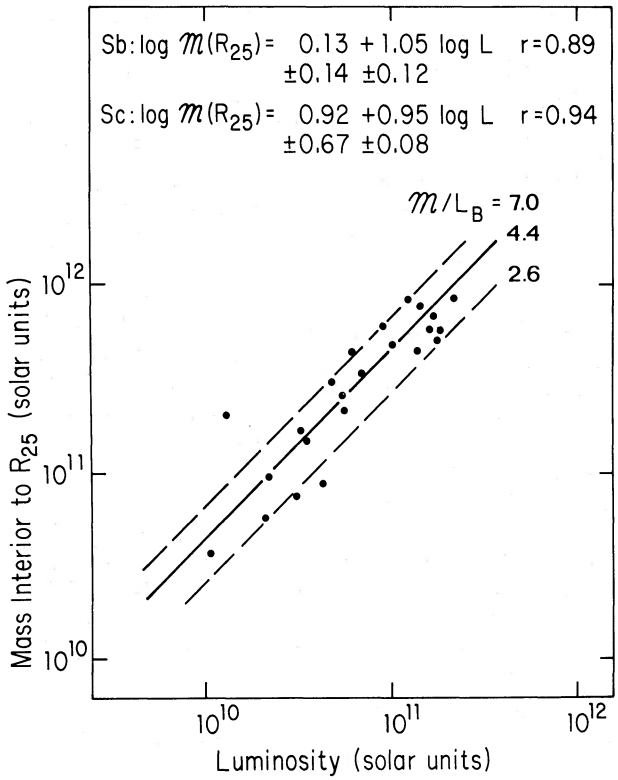

FIG. 8.—Correlation of mass interior to the isophotal radius, $\mathfrak{M}(R_{25})$ with M_B for Sb galaxies (*filled circles*). The least squares fit $\mathfrak{M}(R_{25}) \propto L^{+1.05}$, is indistinguishable from the line $\mathfrak{M}(R_{25})/L_B = 4.4$. Lines of constant $\mathfrak{M}(R_{25})/L_B = 7.0$ and 2.6 are indicated by the dashed lines. The mass-to-blue luminosity ratio is independent of galaxy luminosity over the entire range of luminosity observed for the Sb sample. $\mathfrak{M}(R_{25})/L_B = 2.6$ for the Sc's and 6.1 for the Sa's, both also independent of luminosity.

the values for the Sc's range from 1.4 to 5.3, with a geometric mean of 2.6 ± 0.2.[7]

This difference in average mass-to-blue luminosity ratio between the Sb's and the Sc's has been discussed earlier (Rubin, Ford, and Thonnard 1978; Faber and Gallagher 1979). It is significant, and can be derived in a more fundamental fashion. From equation (1),

$$V^2(R_{25}) = \frac{\mathfrak{M}(R_{25})}{R_{25}} = \frac{\mathfrak{M}(R_{25})}{L_B} \frac{L_B}{R_{25}}.$$

Since the ratio L_B/R_{25} is Hubble-type independent (Fig. 7), one obtains, at a fixed luminosity (or fixed radius),

$$\frac{[V^2(R_{25})]_{\rm Sb}}{[V^2(R_{25})]_{\rm Sc}} = \frac{[\mathfrak{M}(R_{25})/L_B]_{\rm Sb}}{[\mathfrak{M}(R_{25})/L_B]_{\rm Sc}}. \quad (2)$$

At fixed luminosity, $V(R_{25})_{\rm Sb}/V(R_{25})_{\rm Sc} \propto 0.1$ dex (§ IV*a* and Fig. 6*a*). Hence the average mass-to-blue-luminosity ratio of Sb's should be a factor of 0.2 dex = 1.6 higher than that of the Sc's, as is observed ($4.4/2.6 = 1.7$). It also follows from equation (2) that, at equal luminosities, the rotational velocity for an Sb galaxy will be higher than that for an Sc by the square root of the ratio of their mass-to-blue-light ratios, $(4.4/2.6)^{1/2} = 1.3$. At equal masses, the velocity of the Sb will be higher by $(4.4/2.6)^{1/3} = 1.2$.

A least-squares fit of mass with luminosity results in a mean line, $\log \mathfrak{M}(R_{25}) = 0.60 \pm 0.14 + (1.05 \pm 0.12) \log L$, almost indistinguishable from the line $\mathfrak{M}(R_{25})/L_B = \text{constant} = 4.4$ (Fig. 8). The $\mathfrak{M}(R_{25})/L_B$ ratio for Sb galaxies is independent of luminosity, as it is also for the Sc's. *It is remarkable that over a range in luminosity of 20 for the Sb's and 100 for the Sc's, the ratio of mass to blue luminosity is independent of luminosity, but dependent on Hubble type.* Because these correlations contain information related to the history of stellar populations in galaxies, they will be important in setting constraints for evolutionary models.

Mass-to-light ratios in other spectral bands should help to define the stellar populations in spirals, but it is important to remember that both luminosity *and radius* must be measured in the same passband to derive reliable *relative* mass-to-light ratios (Burstein 1982*a*).

[7]Paper II incorrectly quoted a mean $\mathfrak{M}(R_{25})/L_B$ of 3.0 ± 0.3 for 20 Sc galaxies. The correct geometric mean is 2.6 ± 0.2; the individual $\mathfrak{M}(R_{25})/L_B$ values in Paper II are correct. Because of the large uncertainty in the apparent magnitude of UGC 2885, it has been excluded in all Sc galaxy correlations involving luminosity both in Paper II and this paper.

VI. CONCLUSIONS

For a sample of 23 Sb field spirals, we have obtained spectra and determined rotation curves in the mean to $\sim 76\%$ of the isophotal radius (R_{25}). The galaxies span a range in luminosity from 1×10^{10} to 22×10^{10} $L_\odot$, a range in mass from 3.6×10^{10} to 85×10^{10} $\mathfrak{M}_\odot$; and a range in radius from 5 to 51 kpc. The following conclusions follow from an analysis of these data and a comparison of the Sb's with the Sc's studied previously (Papers I and II).

1. Rotation velocities remain high at large nuclear distances for all Sb's observed. No galaxy in the sample shows a Keplerian velocity decrease with increasing R. Sb galaxies, like the Sc's, must have a significant component of highly underluminous mass at large nuclear distances, i.e., a halo.

2. Rotational properties are a function of luminosity within the Sb class. Velocities in small, low-luminosity, low-mass Sb galaxies rise gently to a maximum rotational velocity at a large fraction of the isophotal radius. Velocities in large, high-luminosity, high-mass Sb's reach their (higher) rotational velocity at only a small fraction of the isophotal radius.

3. Many Sb rotation curves share the characteristic form seen in the Sc's. In the range $1 < R < 25$ kpc, $V(R) \propto R^{0.1}$. Hence the dynamical mass rises as $\mathfrak{M}(R) \propto R^{1.2}$ and the local density averaged over a spherical shell falls as $\rho(R) \propto R^{-1.8}$.

4. Isophotal radius and blue luminosity are tightly correlated: $L \propto R^n$, where $n < 2$. Hence, mean surface brightness decreases with increasing luminosity. There is no significant difference in the radius-luminosity correlation in the B band for Sb and Sc spirals.

5. Correlations exist between velocity at the isophotal radius, $V(R_{25})$, and radius; and between $V(R_{25})$ and blue absolute magnitude, M_B, i.e., the conventional Tully-Fisher relations. However, the regression line for Sb galaxies is displaced ~ 0.1 dex from that for Sc's, in both diagrams. At equal luminosity, an Sb has a rotational velocity 1.26 times higher than that of an Sc. At equal rotational velocity, an Sb is both smaller and less luminous than an Sc.

6. The mean slope of the $V(R_{25})$ versus M_B relation is steep (~ -10) for both Sb and Sc galaxies, even with blue magnitudes.

7. At equal luminosity, an Sb will be the same size as an Sc (conclusion 4 above) but have a rotational velocity higher by 0.1 dex (conclusion 5 above). Hence the Sb mass will be higher by $V^2 = 0.2$ dex. At every nuclear distance, an Sb has a higher density than an Sc of equivalent luminosity.

8. The mass (interior to the isophotal radius) to blue luminosity ratio is independent of luminosity within a single Hubble class. The geometric mean, $\langle \mathfrak{M}(R_{25})/L_B \rangle = 4.4 \pm 0.4$ for Sb's; $\langle \mathfrak{M}(R_{25})/L_B \rangle =$

TABLE 4

OBSERVING PARAMETERS FOR GALAXIES IN FIGURE 1

GALAXY (NGC)	DIRECT PLATES					SPECTROGRAMS			
	Telescope[a]	Plate[b]	Filter	Scale (arcsec mm^{-1})	Exposure (minutes)	Telescope[c]	Dispersion (Å mm^{-1})	Scale (arcsec mm^{-1})	Exposure[d] (minutes)
4800	PS	103aO	GG13	67	30	KPNO	25	25	127
2708	L42	IIIaJ*	BG23	11	25	CTIO	25	25	135
3067	L42	IIIaJ*	BG23	11	30	KPNO	25	25	120
4448	PS	098-04	Wr25	67	35	KPNO	25	25	129
1515	Copy of SRC J		...	67	...	CTIO	25	25	151
1353	Copy of ESO B		...	67	...	LC	63	52	129
1325	Copy of ESO B		...	67	...	CTIO	25	25	150
7537	PS	103aO	GG13	67	25	KPNO	25	25	90
U11810	L72	IIIaJ*	BG23	6	15	LC	63	52	135
7171	L42	IIIaJ*	BG23	11	20	LC	63	52	140
7217	PS	103aO	GG13	67	25	KPNO	25	25	120
1620	L42	IIIaJ*	BG23	11	20	KPNO	44	21	130
3054	Copy of ESO B		...	67	...	CTIO	50	25	131
2590	L42	IIIaJ*	BG23	11	15	CTIO	25	25	120
2815	Copy of SRC J		...	67	...	CTIO	25	25	158
1417	L42	IIIaJ*	BG23	11	20	CTIO	25	25	180
1085	L42	IIIaJ*	BG23	11	20	CTIO	25	25	160
7083	Copy of SRC J		...	67	...	LC	63	52	174
U12810	L72	IIIaJ*	BG23	6	15	CTIO	25	25	180
3145	Copy of POSS		...	67	...	CTIO	50	25	90
3223	Copy of ESO B		...	67	...	CTIO	50	25	139
7606	L72	IIIaJ*	BG23	6	15	CTIO	25	25	150
3200	Copy of ESO B		...	67	...	CTIO	50	25	150

[a] PS = Palomar Schmidt; L42 Lowell 42 inch; L72 = Lowell 72 inch.
[b] IIIaJ* = Final phosphor of RCA C33063 Carnegie Image tube imaged with N_2 baked IIIa-J plates.
[c] KPNO = Kitt Peak 4 m; CTIO = Cerro Tololo 4 m; LC = Las Campanas 100 inch.
[d] Final phosphor of RCA C33063 Carnegie image tube imaged with N_2 baked IIIa-J plates which had been preflashed.

2.6 ± 0.2 for the Sc's. (And for the 11 Sa galaxies we are presently studying, $\langle \mathfrak{M}(R_{25})/L_B \rangle = 6.1 \pm 0.7$.)

9. It follows from the above conclusions that two parameters are necessary to define the general dynamical properties of a normal field spiral: these may be Hubble type and luminosity, or a parameter closely correlated with luminosity, which can be radius, or V_{max}, or mass, or density. Of these, density appears to be the most fundamental for models of galaxy formation and evolution.

We thank the Directors of Arecibo Observatory, Cerro Tololo Inter-American Observatory, Kitt Peak National Observatory, Lowell Observatory, National Radio Astronomy Observatory, and Palomar Observatory for telescope time; Drs. Sandra Faber, François Schweizer, and Bradley Whitmore for valuable comments; and the referee, Dr. Jeremy Mould, for reminding us not to stray too far from the observations.

APPENDIX

Reproductions of direct plates and spectrograms of the program galaxies are given in Figure 1 (Plates 4–7). Table 4 gives the observing parameters for these plates.

REFERENCES

Aaronson, M. 1977, Ph.D. thesis, Harvard University.
_____. 1978, *Ap. J.* (*Letters*), **221**, L103.
Aaronson, M., Huchra, J., and Mould, J. 1979, *Ap. J.*, **229**, 1, (AHM).
Aaronson, M, Huchra, J., Mould, J., Schechter, P., and Tully, R. B. 1982, *Ap. J.*, **258**, 64.
Aaronson, M., Mould, J., Huchra, J., Sullivan, W. T., Schommer, R. A., and Bothun, G. D. 1980, *Ap. J.*, **239**, 12.

Bottinelli, L., Gouguenheim, L., Paturel, G., and de Vaucouleurs, G. 1980, *Ap. J.* (*Letters*), **242**, L153.
Brault, J., and Hubbard, R. 1981, private communication.
Brosche, P. 1973, *Astr. Ap.*, **23**, 259.
Bujarrabal, V., Guibert, J., and Balkowski, C. 1981, *Astr. Ap.*, **104**, 1.
Burstein, D. 1982*a*, *Ap. J.*, **253**, 539.
_____. 1982*b*, in preparation..
Burstein, D., and Heiles, C. 1978, *Ap. Letters*, **19**, 69.
_____. 1982, *A.J.*, in preparation.
Burstein, D., Rubin, V. C., Thonnard, N., and Ford, W. K., Jr. 1982, *Ap. J.*, **253**, 70 (Paper II).
Davis, M., Tonry, J., Huchra, J., Latham, D. W. 1980, *Ap. J.* (*Letters*), **238**, L113.
de Vaucouleurs, G. 1959, *A.J.*, **64**, 397.
_____. 1975, in *Galaxies and the Universe*, ed. A. and M. Sandage and J. Kristian (Chicago: University of Chicago Press), p. 557.
_____. 1977, in *Photometry, Kinematics and Dynamics of Galaxies*, ed. D. S. Evans (Austin: University of Texas Astronomy Dept.), p. 1.
de Vaucouleurs, G., de Vaucouleurs, A., and Corwin, H. G. 1976, *Second Reference Catalogue of Bright Galaxies* (Austin: University of Texas Press) (RC2).
Faber, S. M., and Gallagher, J. S. 1979, *Ann. Rev. Astr. Ap.*, **17**, 135.
Haschick, A. D., and Burke, B. F. 1975, *Ap. J.* (*Letters*), **200**, L137.
Morgan, W. W. 1959, *Pub. A.S.P.*, **71**, 394.
Nilson, P. 1973, *Uppsala General Catalog of Galaxies* (Uppsala Obs. Ann., Vol. 6) (UGC).
Peterson, C. J., Rubin, V. C., Ford, W. K., Jr., and Roberts, M. S. 1978, *Ap. J.*, **226**, 770.
Roberts, M. S. 1978, *A.J.*, **83**, 1026.
Rood, H. J. 1980, preprint.
Rubin, V. C., Burstein, D., and Thonnard, N. 1980, *Ap. J.* (*Letters*), **242**, L149.
Rubin, V. C., Ford, W. K., Jr., and Thonnard, N. 1978, *Ap. J.* (*Letters*), **225**, L107.
Rubin, V. C., Ford, W. K., Jr., and Thonnard, N. 1980, *Ap. J.*, **238**, 471 (Paper I).
Rubin, V. C. Thonnard, N., and Ford, W. K., Jr. 1982, *A.J.*, **87**, 477.
Rubin, V. C., Thonnard, N., Ford, W. K., Jr., and Roberts, M. 1976, *A.J.*, **81**, 719.
Sandage, A. 1961, *The Hubble Atlas of Galaxies* (Washington: Carnegie Institution of Washington).
Sandage, A., and Tammann, G. A. 1981, *A Revised Shapley-Ames Catalog of Bright Galaxies* (Washington: Carnegie Institution of Washington) (RSA).
Schechter, P. 1980, *A.J.*, **85**, 801.
Thonnard, N., Roberts, M., Ford, W. K., Jr., and Rubin, V. C. 1982, in preparation.
Thonnard, N., and Rubin, V. C. 1981, *Carnegie Yrbk*, **80**, 551.
Thonnard, N., Rubin, V. C., and Ford, W. K., Jr. 1981, *Bull. AAS*, **13**, 507.
Tully, R. B., and Fisher, J. R. 1977, *Astr. Ap.*, **54**, 661 (TF).
Tully, R. B., Mould, J. R., and Aaronson, M. 1982, *Ap. J.*, **257**, 527.
van den Bergh, S. 1960, *Ap. J.*, **131**, 215.
_____. 1961, *Ap. J.*, **131**, 558.
Visvanathan, N. 1981, *Astr. Ap.*, **100**, L20.
Weekes, T. C. 1981, *A.J.*, **86**, 1415.
Whitmore, B. C. 1982, in preparation.

DAVID BURSTEIN: National Radio Astronomy Observatory, Edgemont Road, Charlottesville, VA 22901

W. KENT FORD, JR., VERA C. RUBIN, and NORBERT THONNARD: Department of Terrestrial Magnetism, Carnegie Institution of Washington, 5241 Broad Branch Road, N.W., Washington, DC 20015

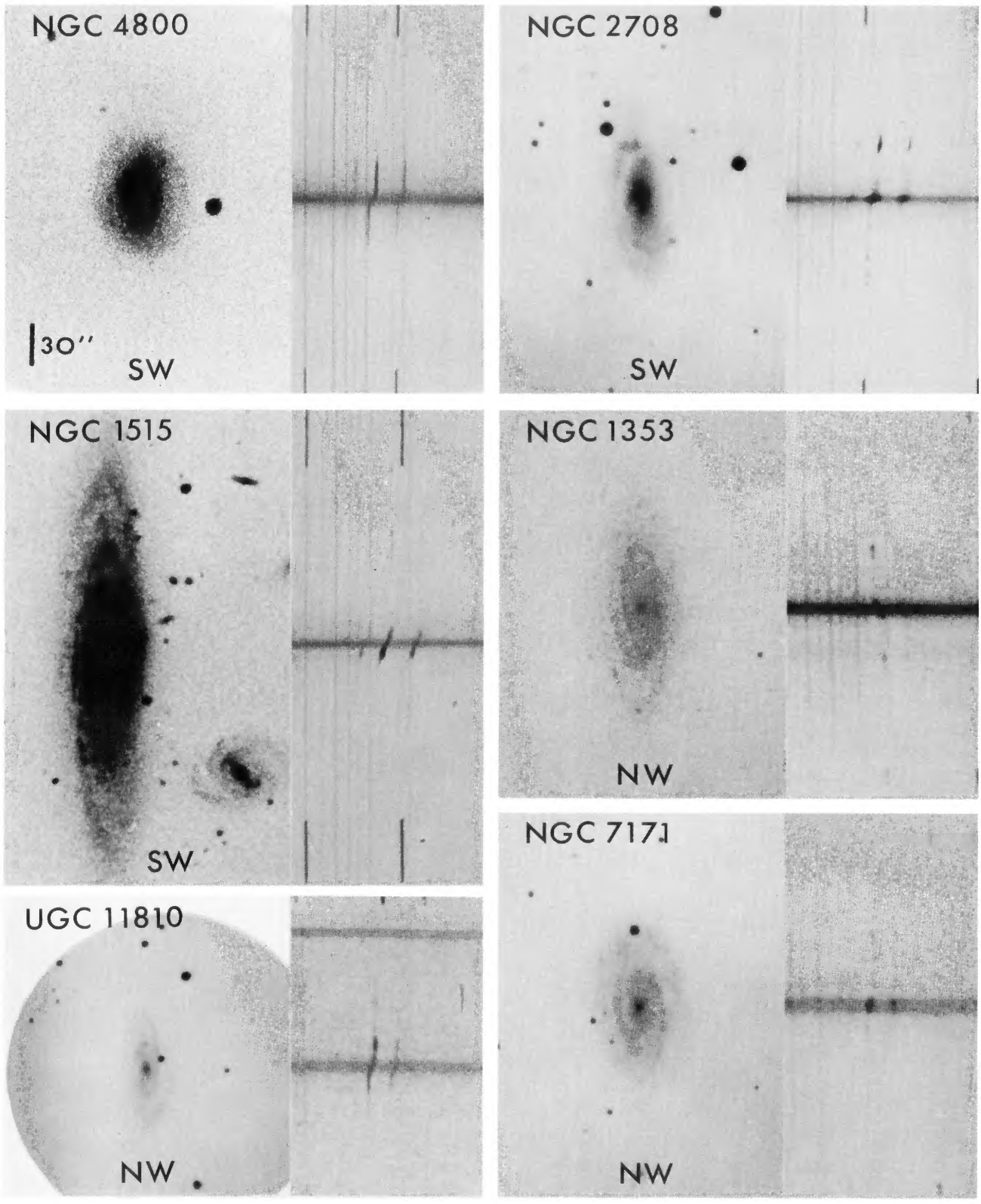

FIG. 1*a*

FIG. 1.—Copies of direct plates and spectrograms for Sb galaxies in study. Details of plate material are listed in Table 4. All galaxies and spectra are printed here to the same angular scale. On each spectrum, the strongest line is Hα, flanked by two [N II] lines, The weak undistorted lines crossing the spectra are night sky OH lines. Galaxies are arranged by increasing luminosity, read from left to right across double page.

RUBIN *et al.* (*see* page 455)

PLATE 5

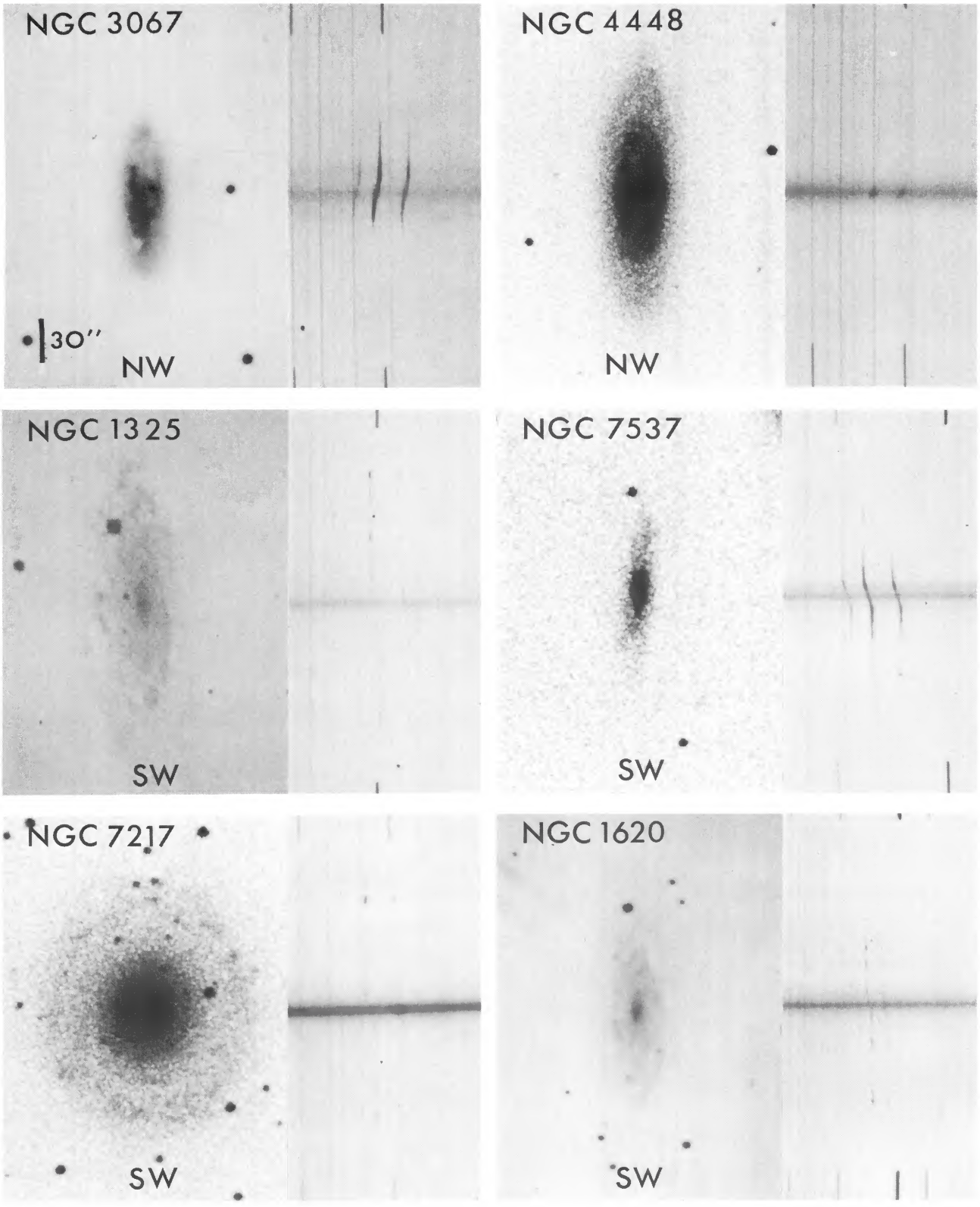

FIG. 1*b*

RUBIN *et al.* (*see* page 455)

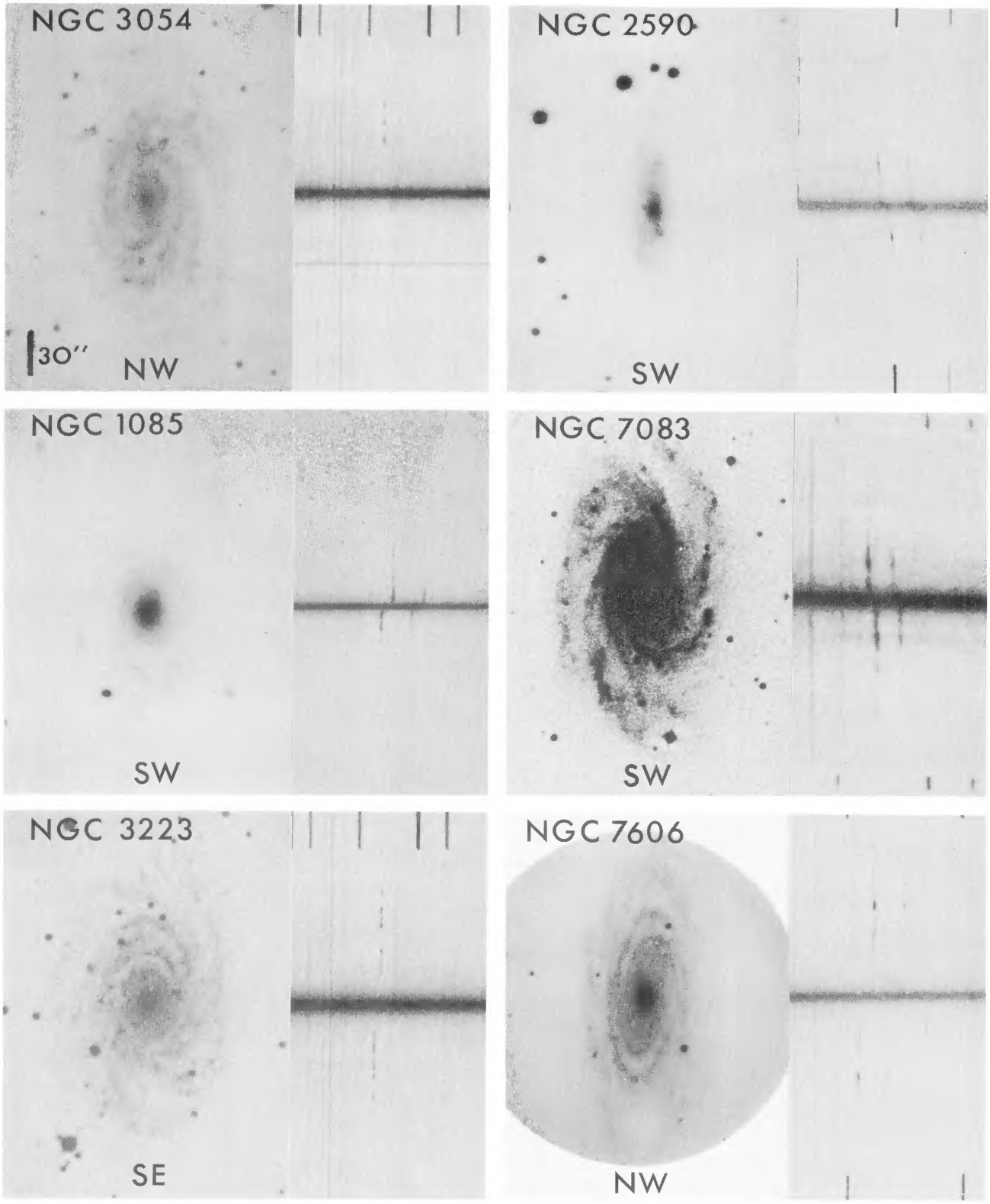

FIG. 1*c*

RUBIN *et al.* (*see* page 455)

PLATE 7

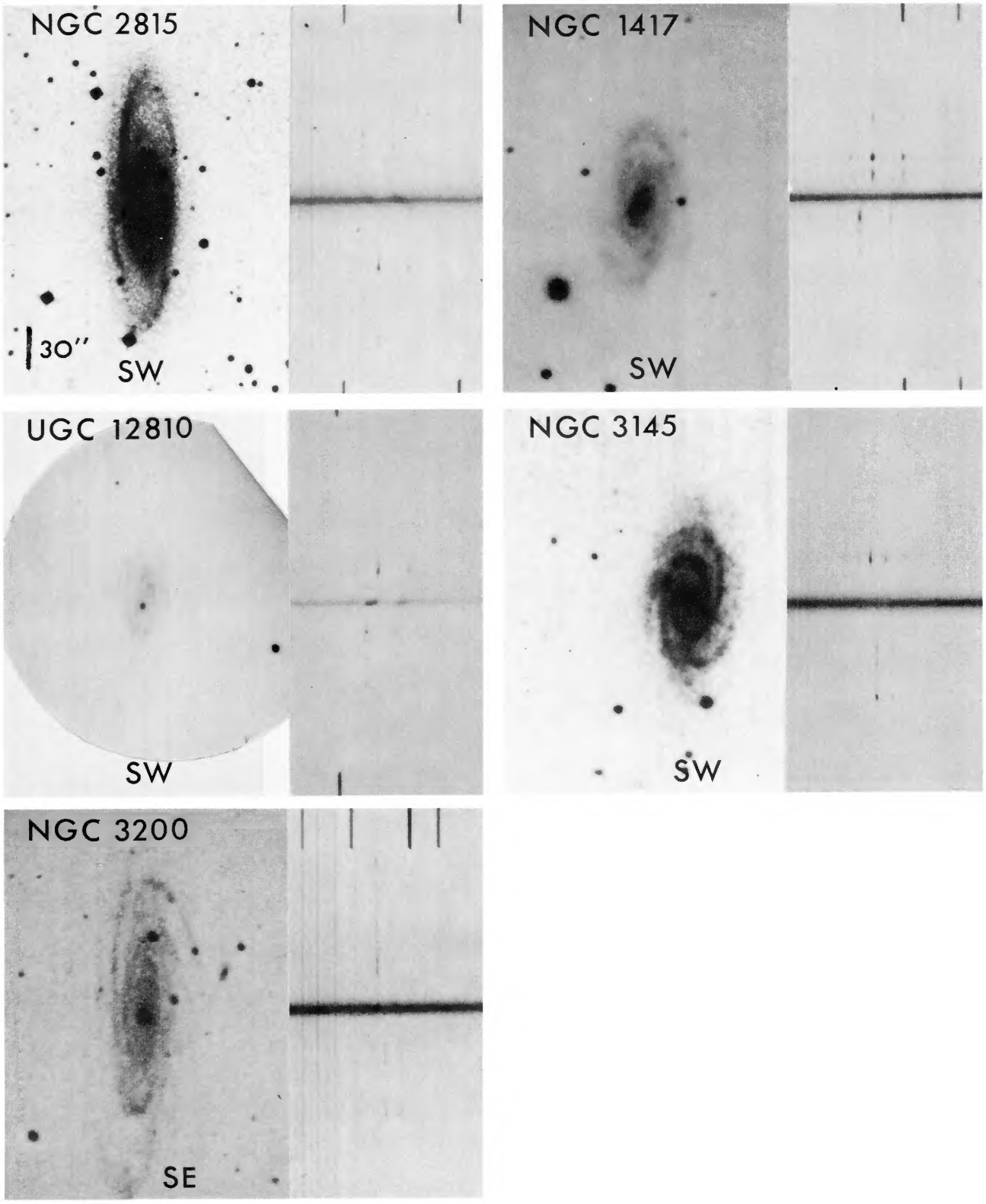

FIG. 1*d*

RUBIN *et al.* (*see* page 455)